Dual-baseline Polarimetric SAR Tomography for Tree Height Estimation Using Single-Pass L-Band PolInSAR Data

Yue Huang, Qiaoping Zhang, Marcus Schwaebisch
Ming Wei, Bryan Mercer

Jan, 2013

Outlines

- Objectives
- System
- Data processing
  - Wavenumber-domain
  - Time-domain
- Methodology for tree height estimation
  - Dual-baseline SAR tomography
- Results
  - Underlying ground and tree top heights
  - Compared with single-baseline PolInSAR inversion techniques
  - Validation against Lidar data
- Conclusion

Rationale and Objectives

- Climate change context:
  - 4 billion ha (30%) of global land cover is forested
  - Within these forests about 72 t/ha carbon are sequestered in above-ground biomass (global mean)
  - *Forest destruction believed responsible for almost 20% of CO2 annual emissions*
    - *Greater than the total transport industry contribution globally*

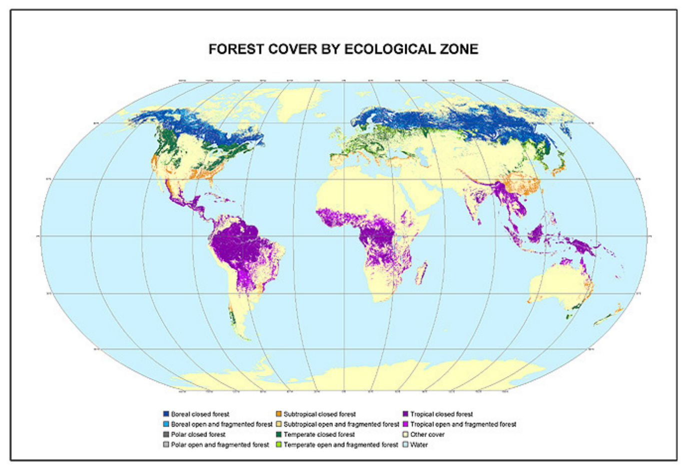

Rationale and Objectives (Cont'd)

- Baseline biomass measurements require improvement in:
  - spatial resolution (to 0.5 ha)
  - coverage (particularly the tropics)
  - accuracy (goal 20%)
- Objective of this work is to demonstrate biomass measurement with single-pass airborne L-Band Pol-InSAR

Single-pass L-Band PolInSAR System

Peak power	0.4 kW
Wavelength	0.2262 m
Polarization	quad (HH, HV, VH, VV)
PRF (per channel)	2200 Hz
max. system bandwidth	up to 135 MHz (80 MHz nominally)
range resolution	up to 1.1 m
azimuth resolution	0.25 m
typical flight altitude	1000 m
swath width	1.2 km
interferometric baseline	3.5 m
NESZ	< -40dB

- Assembled in 2007
- Gulfstream Commander platform
- Radar hardware based on previous X- and P-Band TopoSAR system
- Antennas mounted on rigid beam passing through the un-pressurized part of the fuselage

Data processing

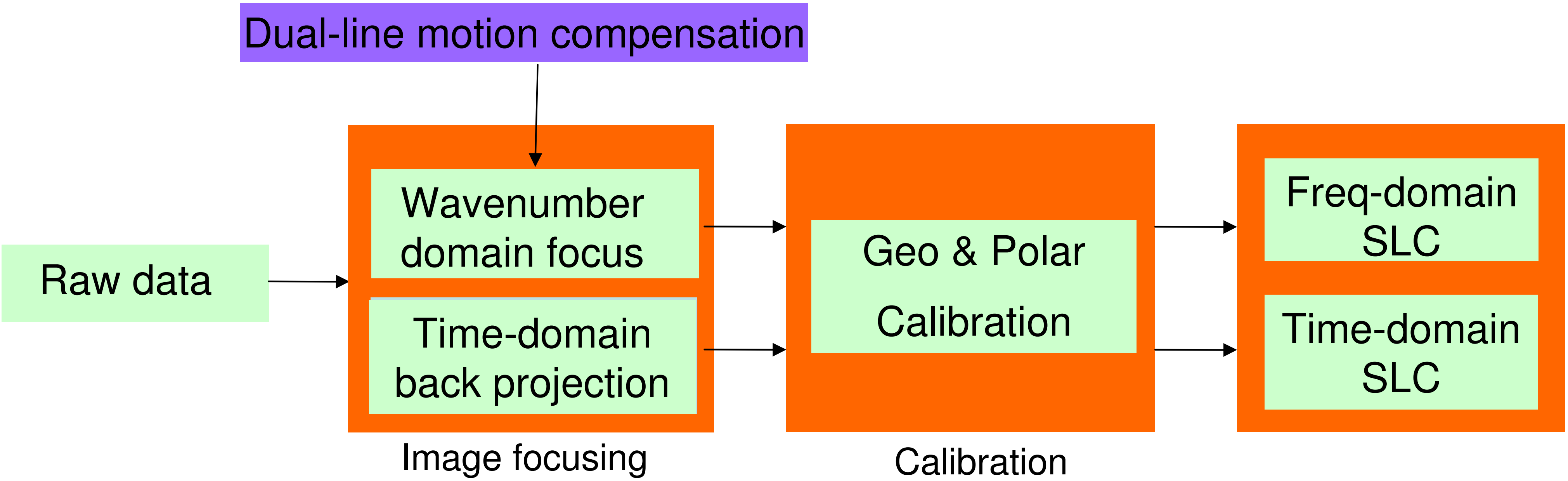

- Focusing performance
  - Interferometric performance, channel mis-registration, coherence (Schwaebisch et al, IGARSS 2010)
  - Tomographic focusing

Single-pass Dual-baseline Possibility

- In our experimental L-Band system, pulses were recorded in both ping-pong and non ping-pong modes simultaneously.
  - →12 active channels were recorded
- This provided three independent antenna phase center positions (noted as NN-NF-FF) in a single flight.
  - →Dual-baseline configuration

Dual-baseline Configuration

Full Baseline: NN-FF

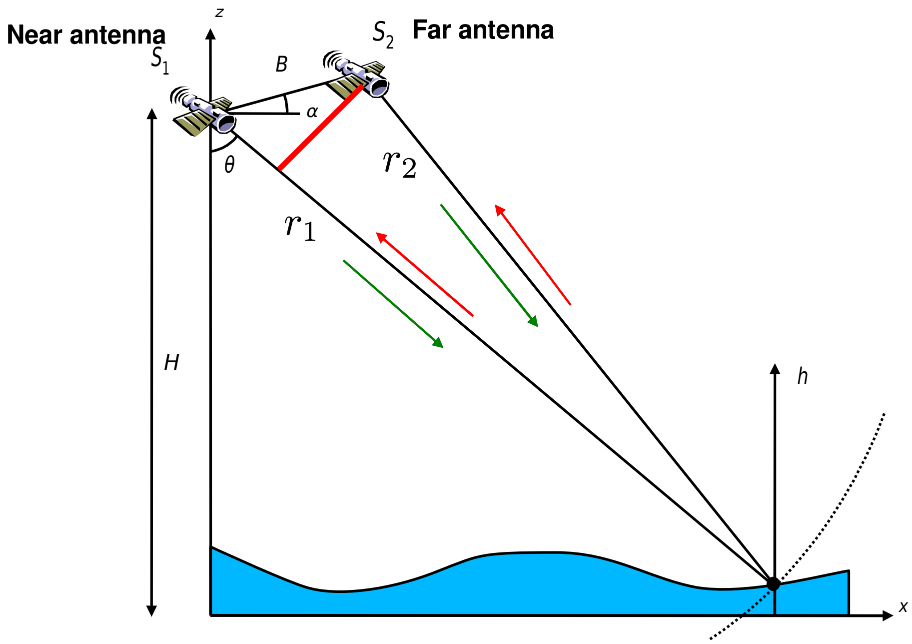

$$\phi_{nn,ff} = \frac{4\pi}{\lambda}(r1 - r2)$$

Half Baseline: NN-NF

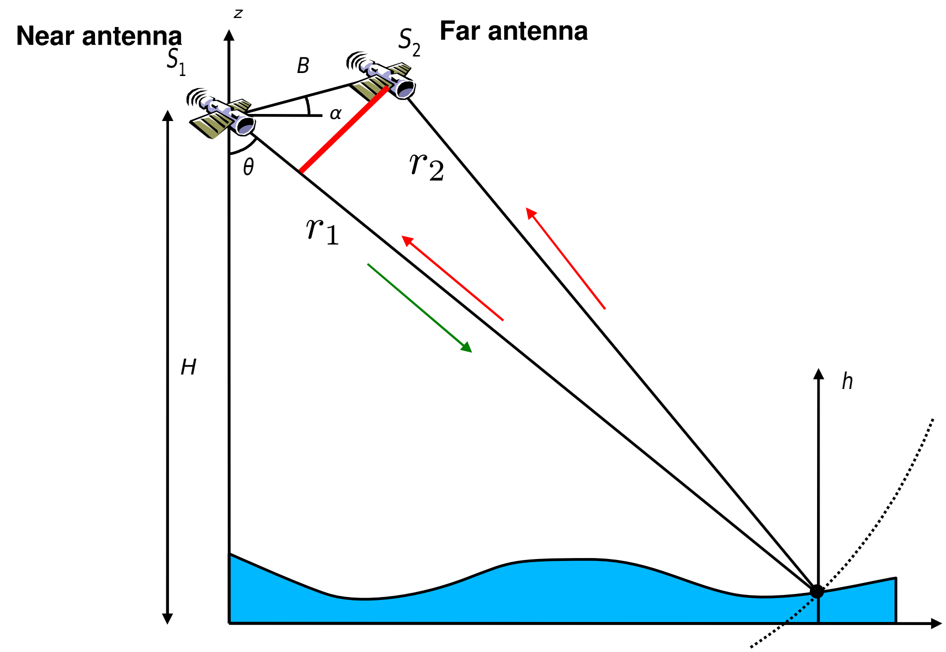

$$\phi_{nn,nf} = \frac{2\pi}{\lambda}(r1 - r2)$$

$$\phi_{nn,ff} = 2\phi_{nn,nf}$$

Dual-baseline PolInSAR Signal Model

Single source

- POLSAR unitary target vector

$$\mathbf{k} = [k_1, k_2, k_3]^T, \; \mathbf{k}^\dagger \mathbf{k} = 1$$

- Polarimetric steering vector

$$\mathbf{a}(z, \mathbf{k}) = \mathbf{k} \otimes \mathbf{a}(z)$$

- 3-M element MB-POLinSAR signal

$$\mathbf{y}_P(l) = \begin{bmatrix} \mathbf{y}_1(l) \\ \mathbf{y}_2(l) \\ \mathbf{y}_3(l) \end{bmatrix} = s(l)\mathbf{a}(z, \mathbf{k}) + \mathbf{n}(l)$$

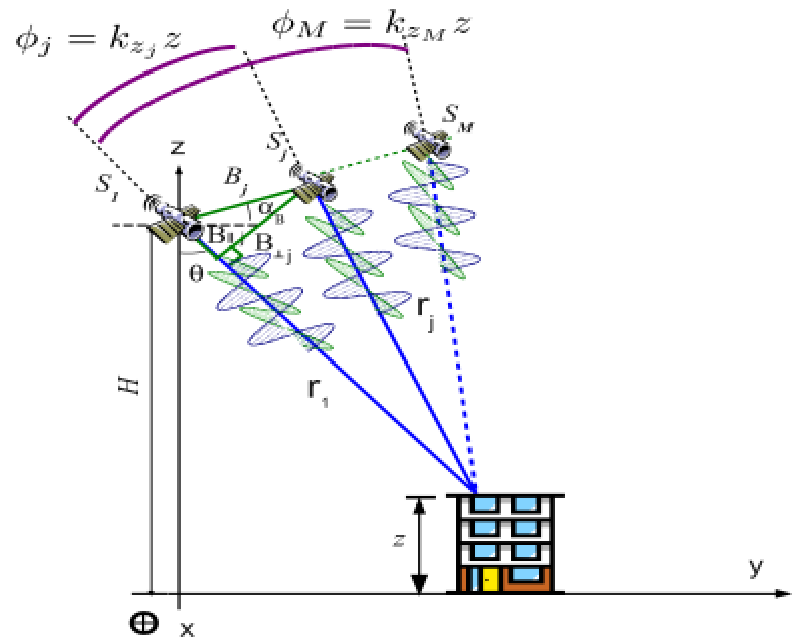

D sources

- Polarimetric steering matrix

$$\mathbf{A}(\mathbf{z}, \mathbf{K}) = [\mathbf{a}(z_1, \mathbf{k}_1), \ldots, \mathbf{a}(z_D, \mathbf{k}_D)]$$

- 3-M element MB-POLinSAR signal

$$\mathbf{y}_P = \mathbf{A}(\mathbf{z}, \mathbf{K})\mathbf{s} + \mathbf{n}$$

$$\mathrm{R} = \frac{1}{L} \sum_{1}^{L} \mathbf{y}_P(l) \mathbf{y}_P^\dagger(l)$$

Polarimetric Tomographic Techniques

- FP-Beamforming:

$$P(z) = \frac{\lambda_{max}(\mathbf{B}^H(z)\mathbf{R}\mathbf{B}(z))}{m^2} \qquad \mathbf{B}(z)^H\mathbf{R}\mathbf{B}(z)\mathbf{k}_{max} = \lambda_{max}\mathbf{k}_{max}$$

- FP- Capon:

$$P(z) = \frac{1}{\lambda_{min}(\mathbf{B}^H(z)\mathbf{R}^{-1}\mathbf{B}(z))} \qquad \mathbf{B}(z)^H\mathbf{R}^{-1}\mathbf{B}(z)\mathbf{k}_{min} = \lambda_{min}\mathbf{k}_{min}$$

- FP-Music:

$$P(z) = \frac{1}{\lambda_{min}(\mathbf{B}^H(z)\mathbf{E}_n\mathbf{E}_n^H\mathbf{B}(z))} \qquad \mathbf{B}(z)^H\mathbf{E}_n\mathbf{E}_n^H\mathbf{B}(z)\mathbf{k}_{min} = \lambda_{min}\mathbf{k}_{min}$$

$$\mathbf{B}(z) = \begin{bmatrix} \mathbf{a}(z) & 0 & 0 \\ 0 & \mathbf{a}(z) & 0 \\ 0 & 0 & \mathbf{a}(z) \end{bmatrix}$$

Elevation: $\hat{\mathbf{z}} = \arg\max P(z)$

Scattering mechanism: $\mathbf{k}_{min}$ or $\mathbf{k}_{max}$

Global view of test sites

INTERMAP TECHNOLOGIES

Test Site: Edson

- Test area near Edson: a forested region of Alberta, Canada
  - Patchwork of lodgepole pine forest and clearcut areas
  - Clearcuts may have been re-planted and in a regrowth phase
  - Typically 15-30 m high
  - L-Band data acquired in Nov. 2007 and again in June 2008
- Ancillary data
  - X-Band DSM (from 2006)
  - Lidar ground elevations and point cloud (courtesy Terrapoint Canada)
  - Color air photo (Valtus)

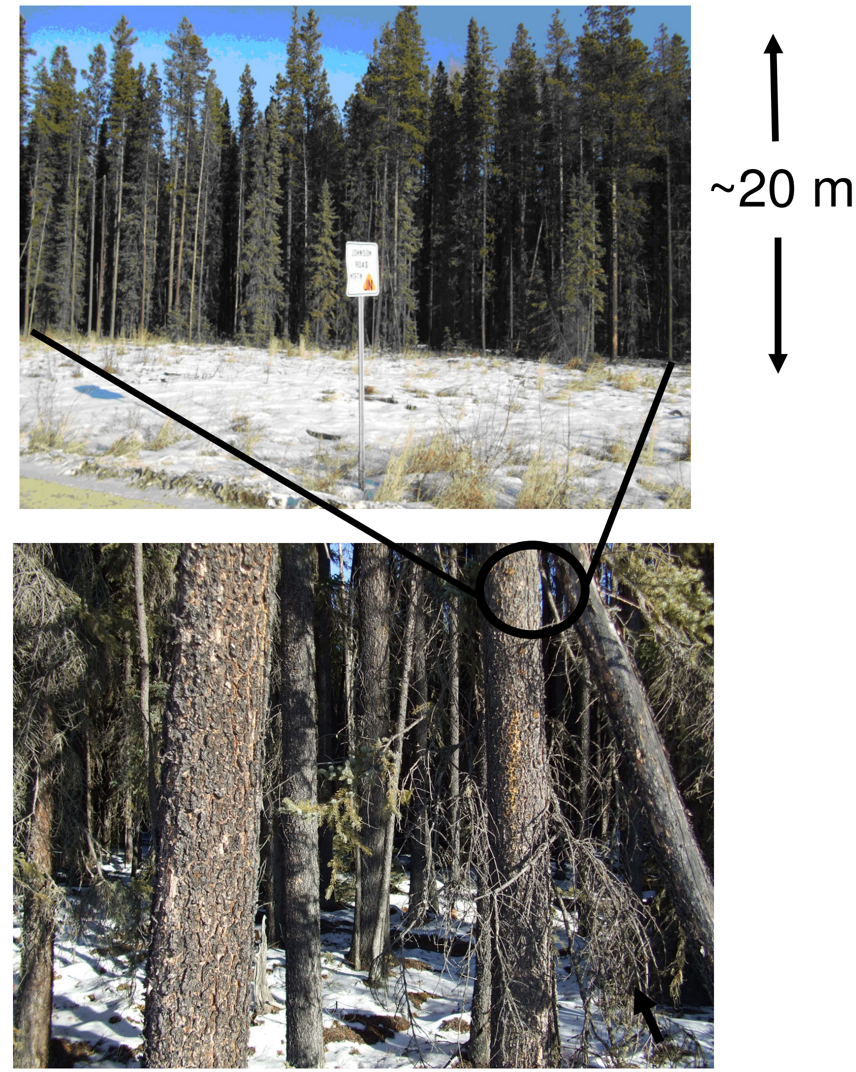

Tomographic techniques for tree estimation

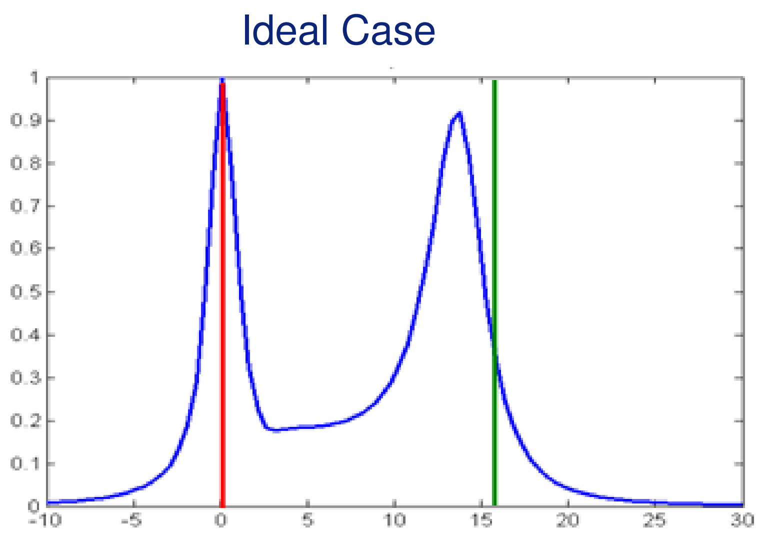

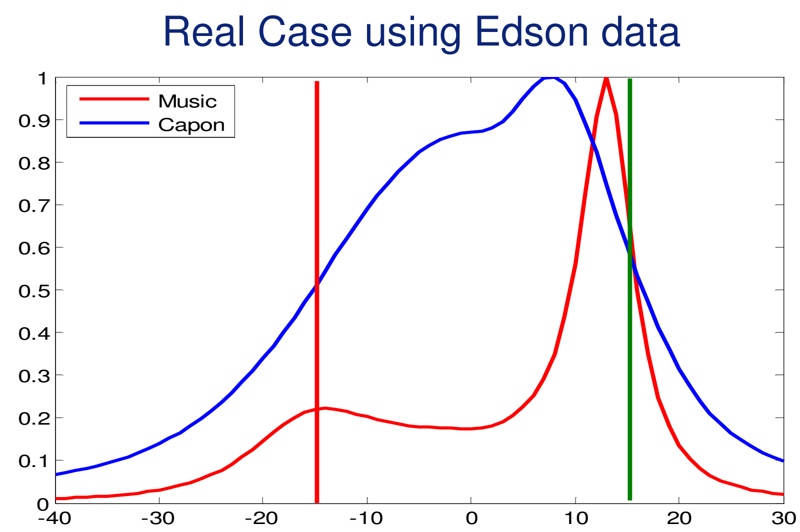

- In our real dual-baseline case, Capon's method merged ground and volume contributions in vertical direction;
- Combining Capon and MUSIC estimators
  - MUSIC: separate ground and volume centers: z_g
  - Capon: approximate the vertical distribution of scatterers,

    truncate tree top height at -3dB from the volume center: z_{top}

Forest/Nonforest mask for tomographic processing

Pauli map

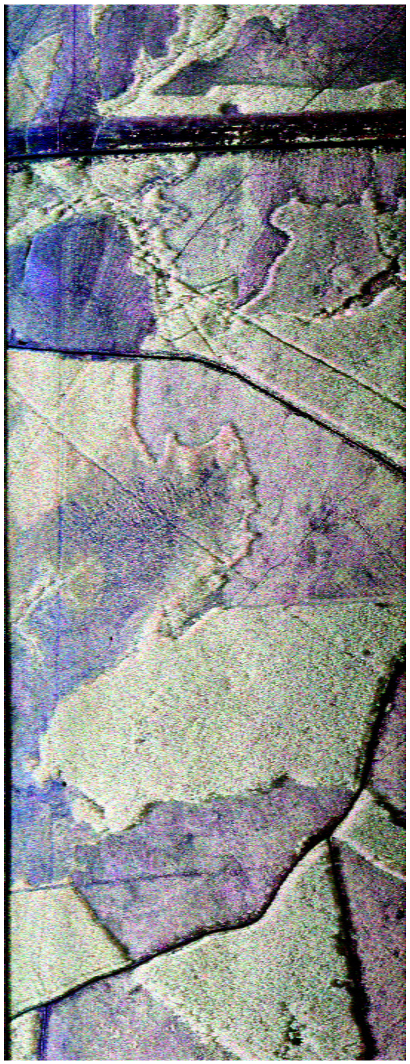

Lidar Tree height map

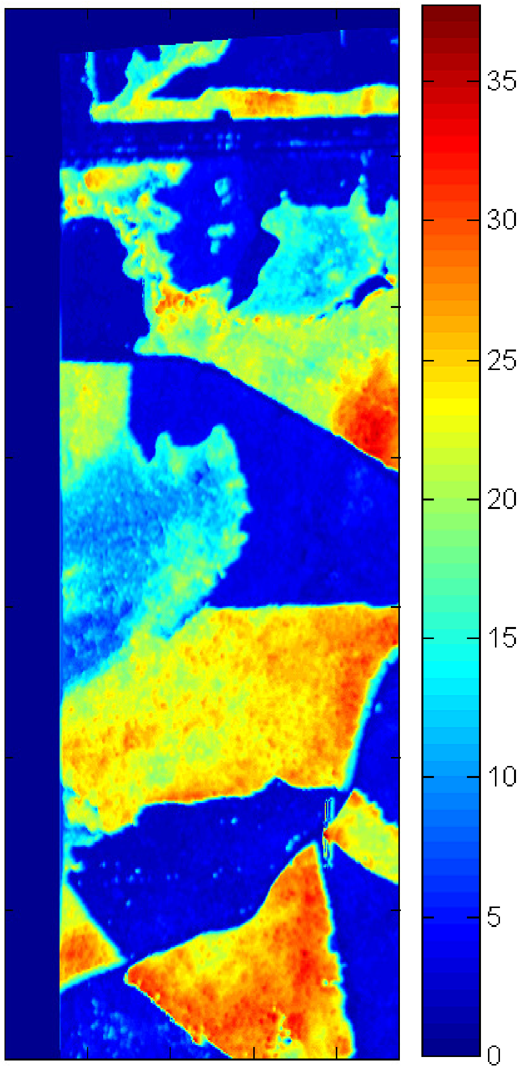

Lidar Hv > =10m

TD data: coh1.mag<0.93

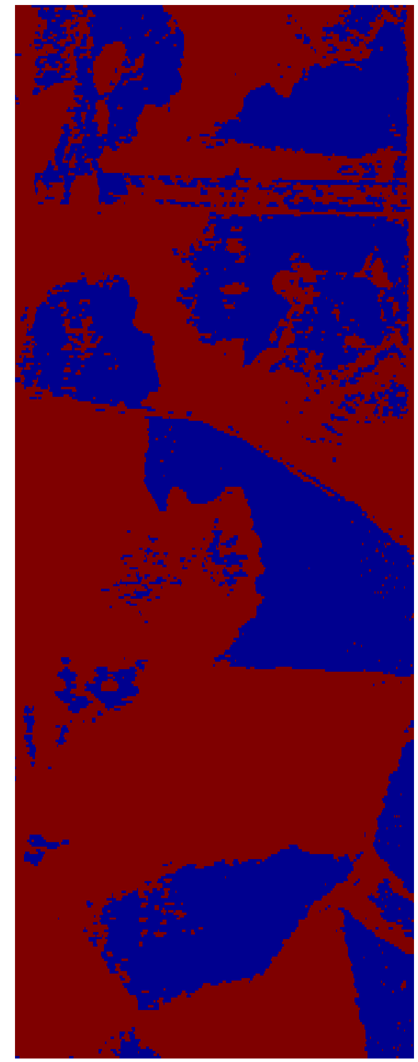

- Focus on trees higher than 10m, mask out short vegetations
- Tomographic processing: order=1, bare; order=5, forested

Results at Near Range

Pauli-coded

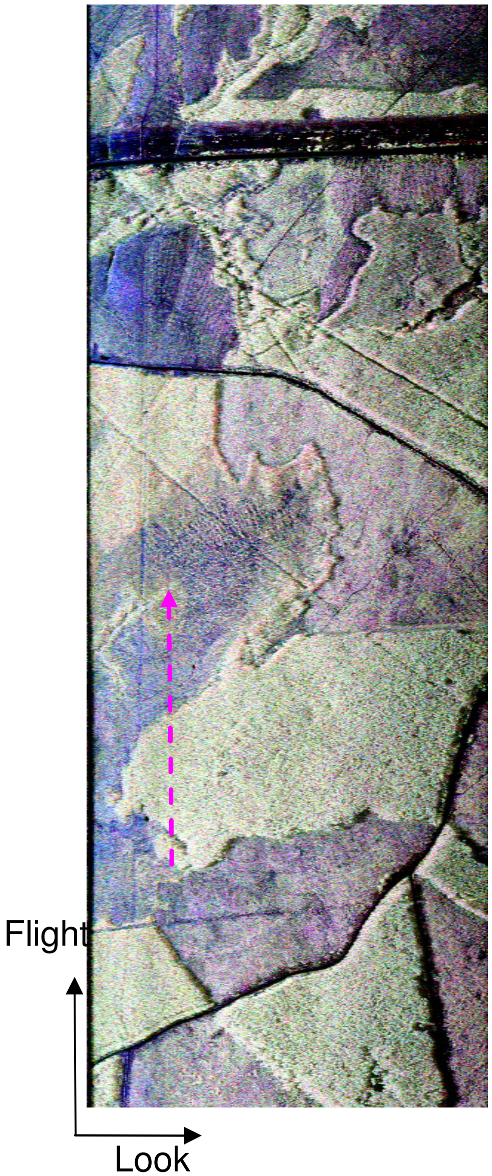

Freq-domain data

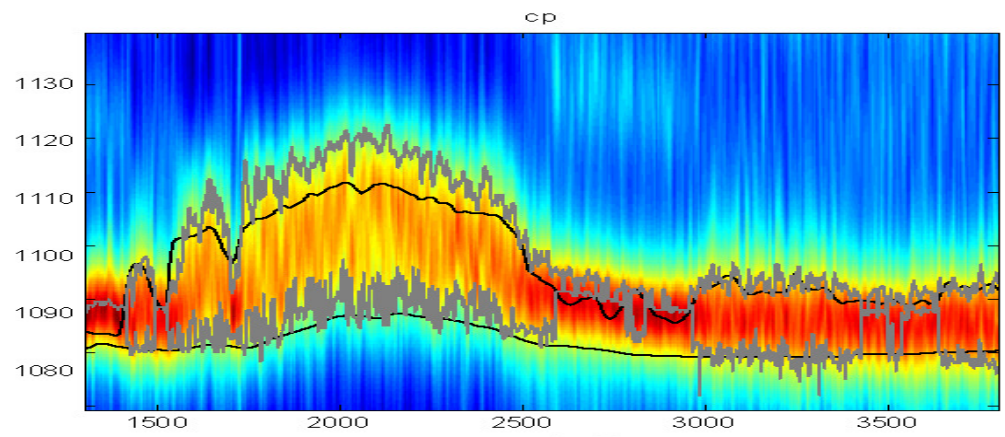

Time-domain data

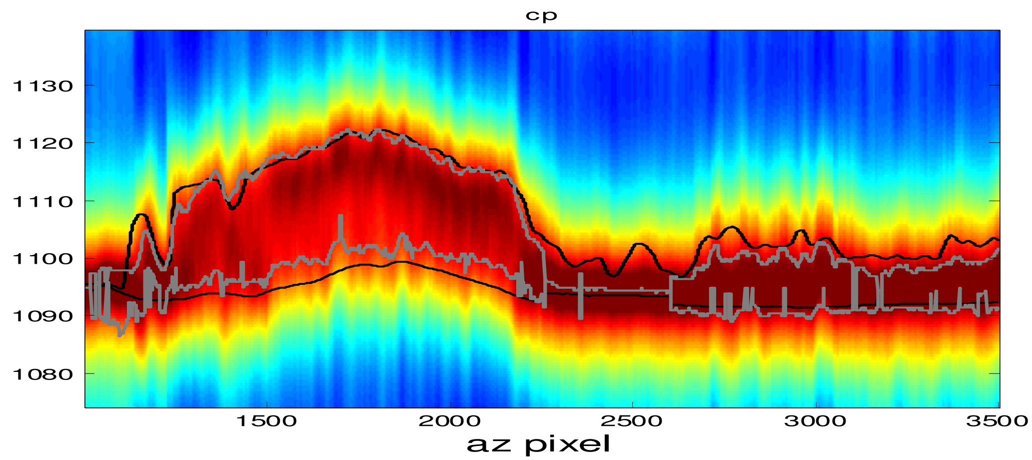

Black lines: LiDAR

Gray lines: SARTomo

Time-domain data provides more stable and precise estimates for ground and tree top.

Results at Mid-Far Range

Pauli-coded

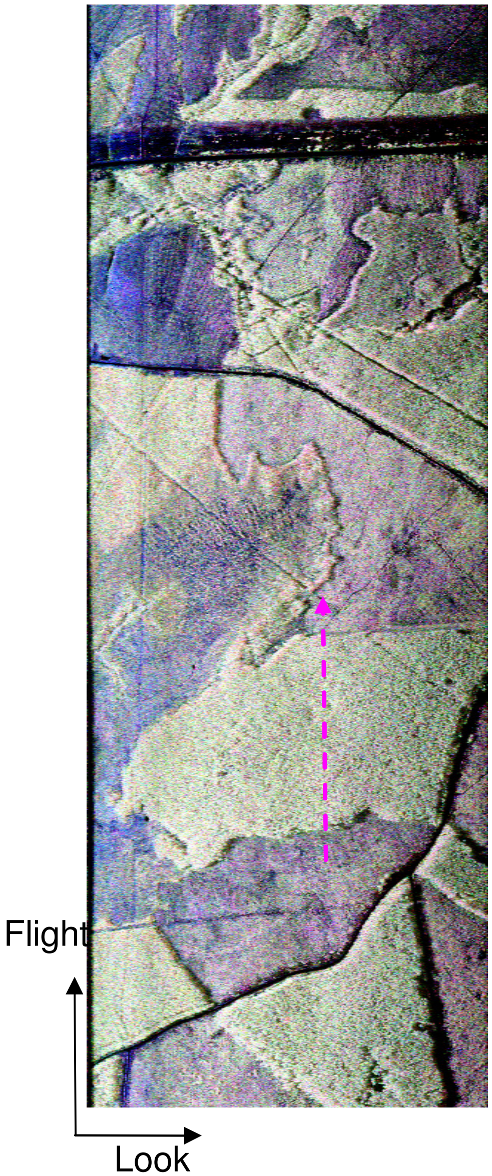

Freq-domain data

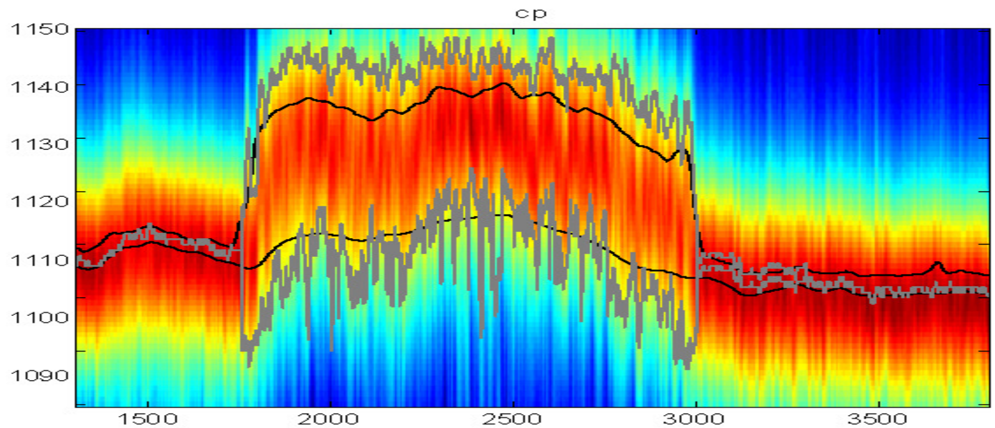

Time-domain data

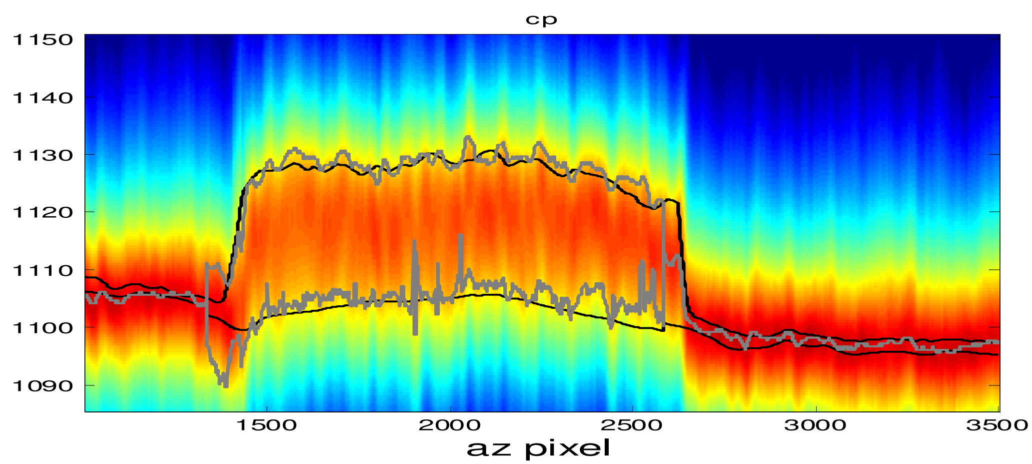

Black lines: LiDAR

Gray lines: SARTomo

Time-domain data provides much better tomographic focusing

Results at Far Range

Pauli-coded

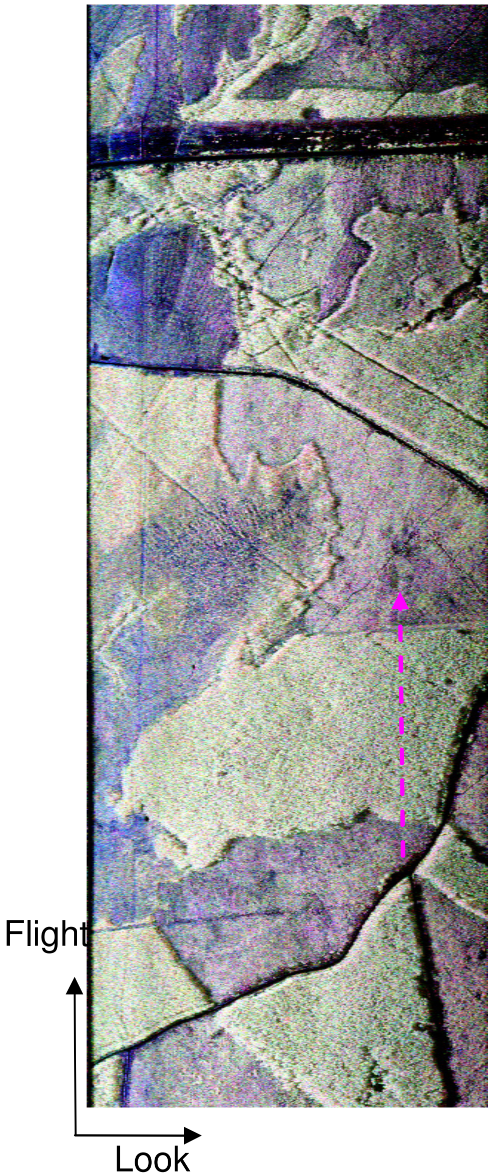

Freq-domain data

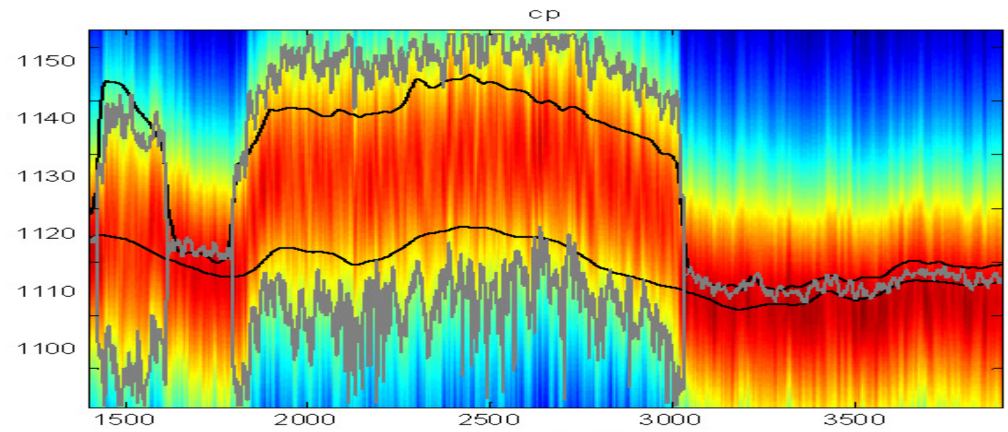

Time-domain data

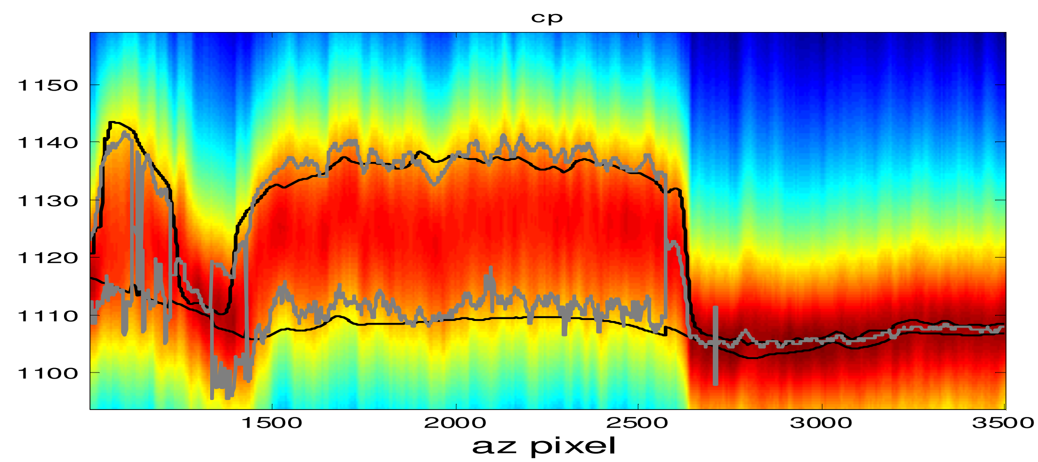

Black lines: LiDAR

Gray lines: SARTomo

Test zone

Airphoto

Lidar DTM

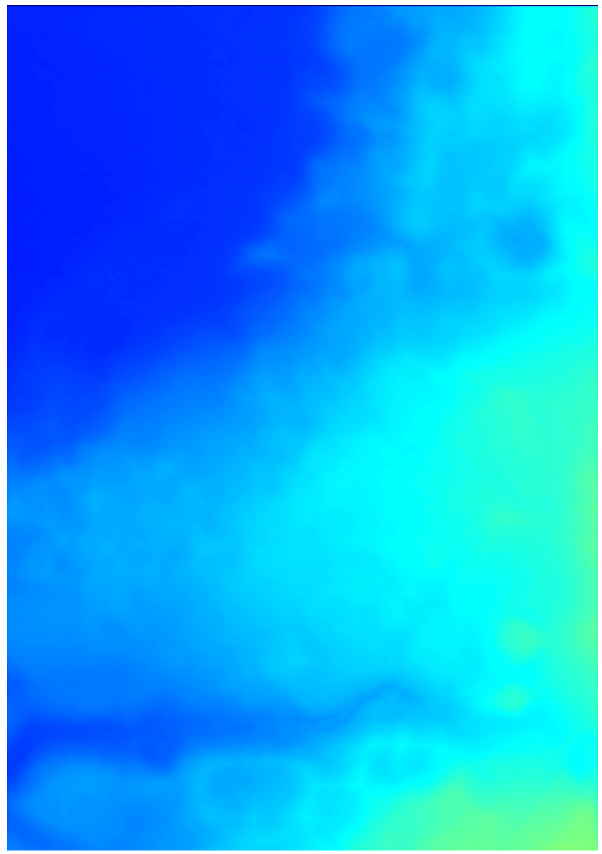

Lidar DSM

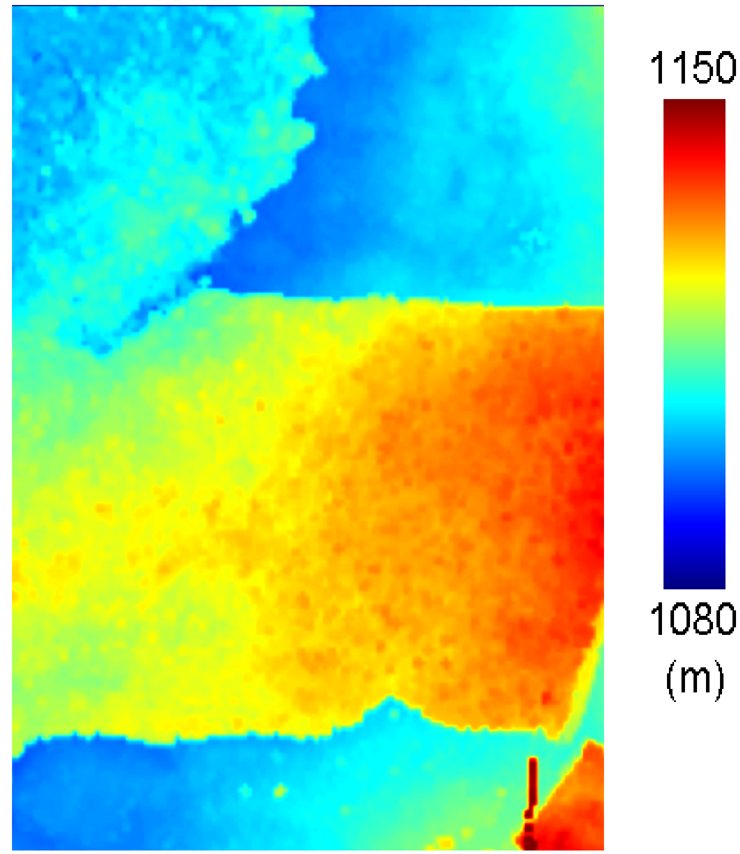

Georeferenced results from T-D data

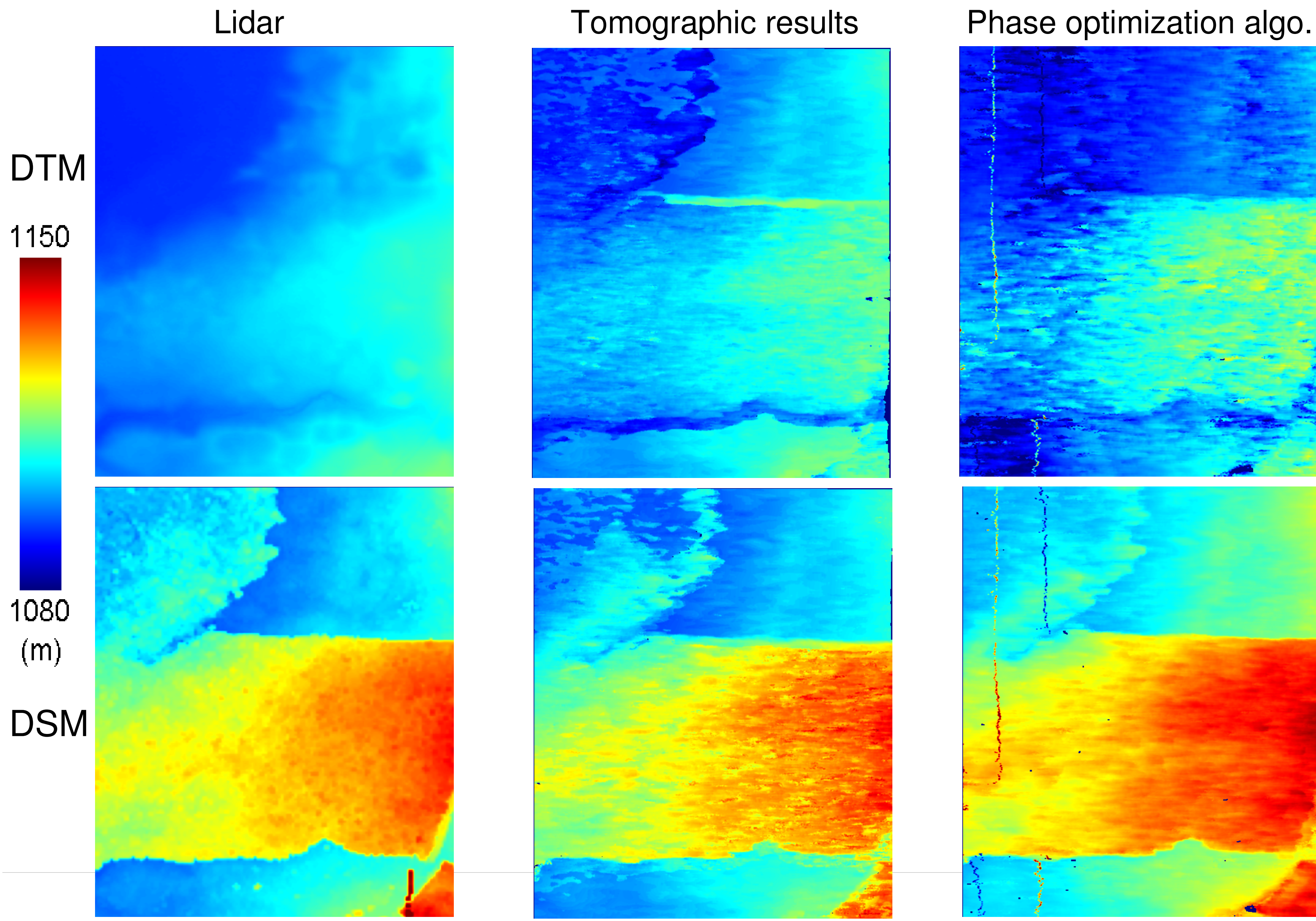

Difference maps for DTM

Tomo DTM-Lidar DTM

Pha.opt DTM-Lidar DTM

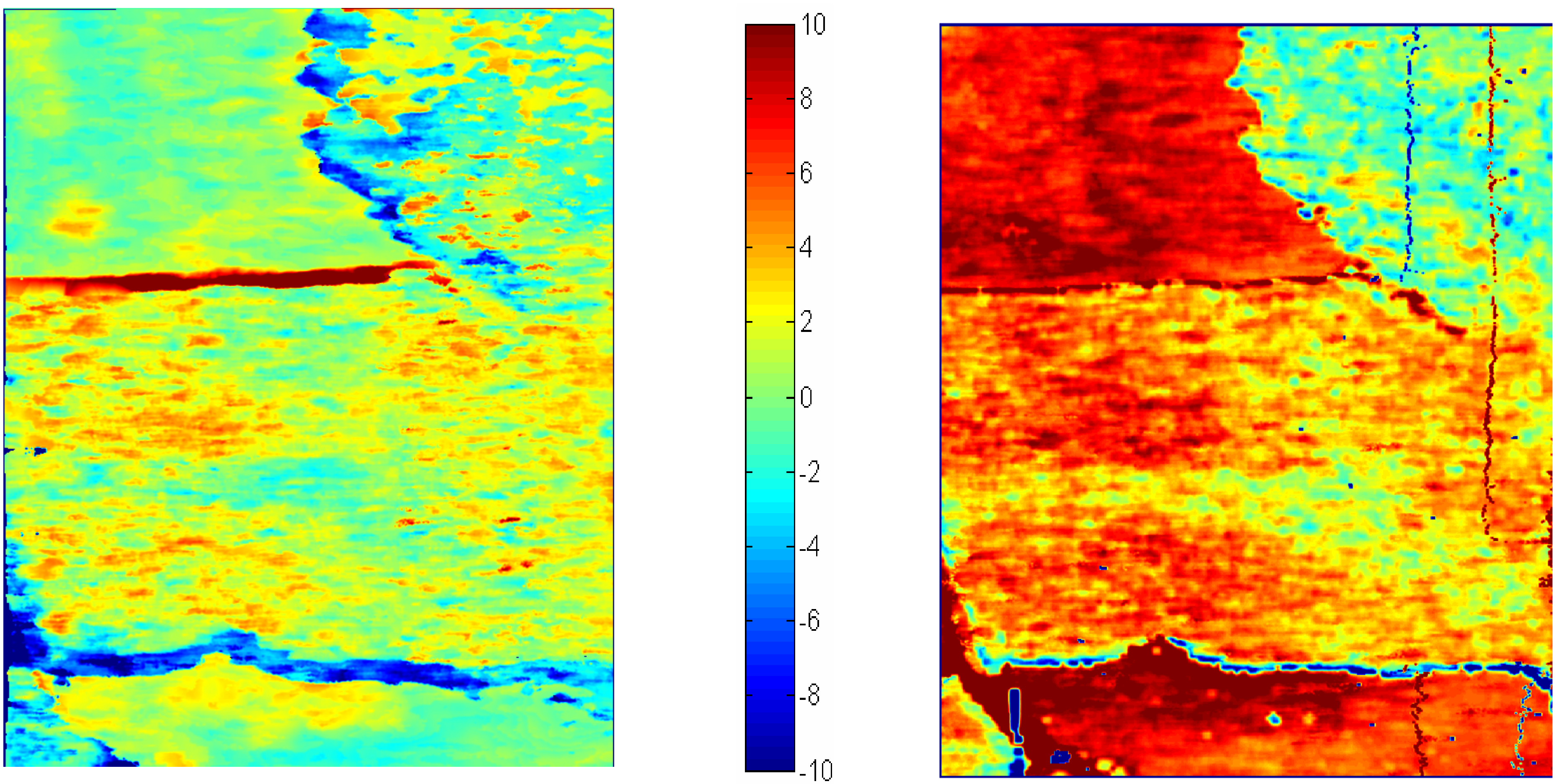

INTERMAP TECHNOLOGIES

Difference maps for DTM

Tomo DTM-Lidar DTM

Pha.opt DTM-Lidar DTM

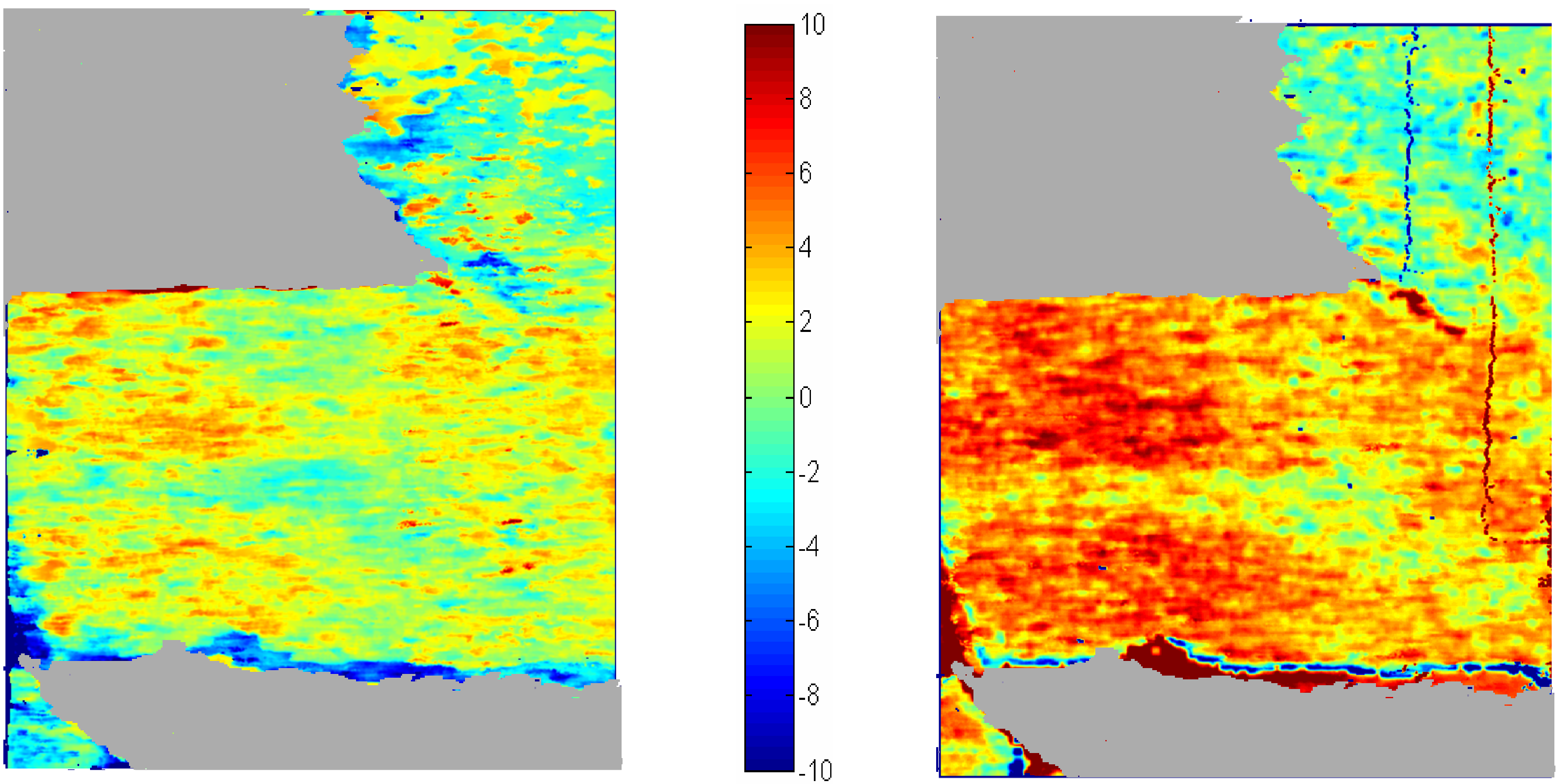

Mask out bare areas, compare forested areas

Tomographic techniques have less overestimation for underlying ground

Difference maps for DSM

Tomo DSM-Lidar DSM

Pha.opt DSM-Lidar DSM

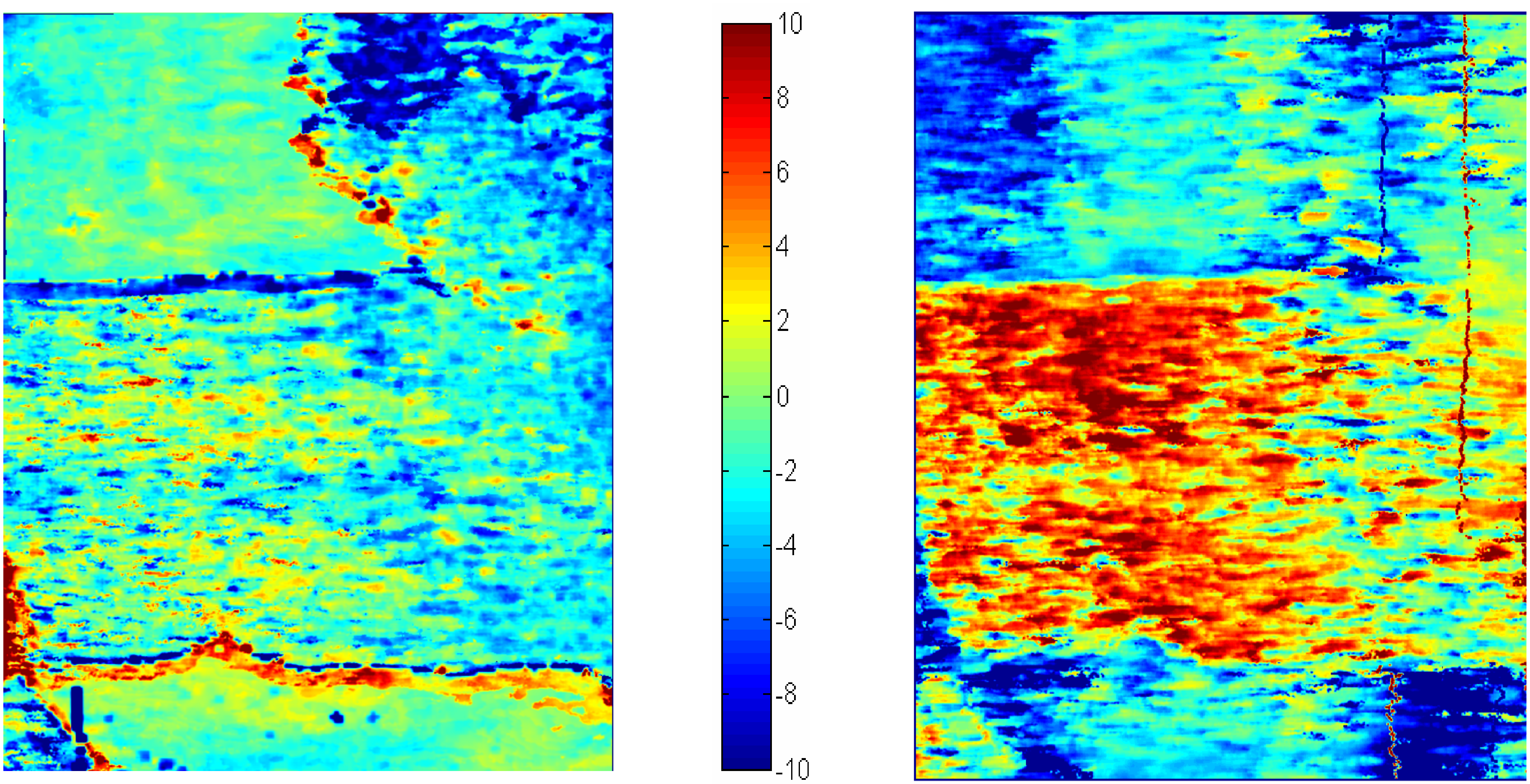

Difference maps for DSM

Tomo DSM-Lidar DSM

Pha.opt DSM-Lidar DSM

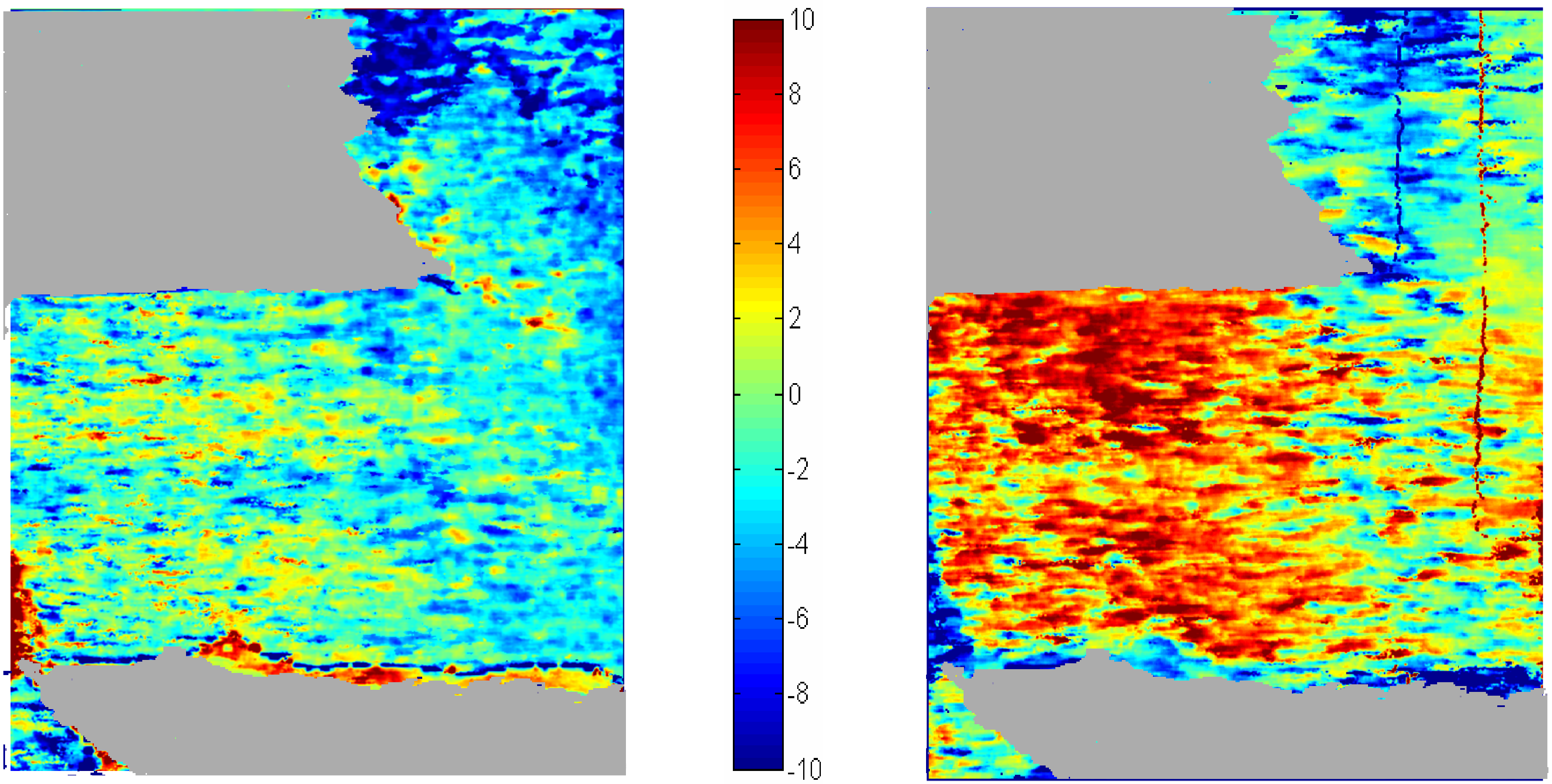

Mask out bare areas, compare forested areas

Tomographic techniques better than phase opt algorithms for tree top heights

Dif DTM=Tomo DTM-Lidar DTM

Dif DSM=Tomo DSM-Lidar DSM

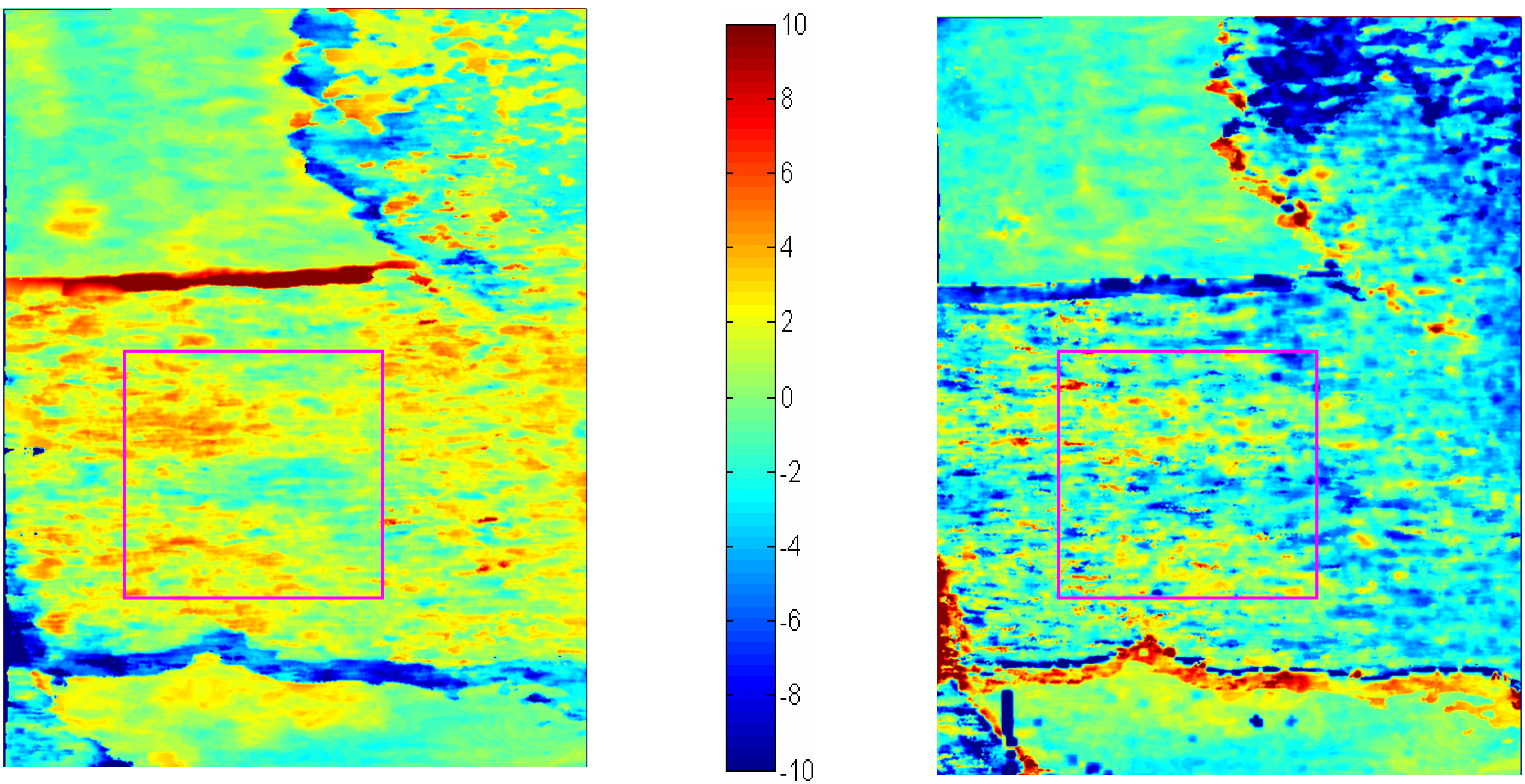

	Mean (m)	STD(m)
Dif DTM	2.58	1.65
Dif DSM	0.12	2.40

Summary and Outlook

- We can potentially obtain better results using dual-baseline SAR tomography, in terms of ground elevation recovery and tree height estimation.
- The system suffered from multi-path affects, which makes both geometric and polarimetric calibration challenging.
- The L-band dual-baseline configuration makes tomographic techniques challenging for the ground elevation estimation.

Acknowledgement

Alberta Innovates Technology Futures